



Parathyroid hormone controls paracellular Ca^{2+} transport in the thick ascending limb by regulating the tight-junction protein Claudin14

Tadatoshi Sato^{a,b}, Marie Courbebaisse^{a,c,1}, Noriko Ide^{a,1}, Yi Fan^a, Jun-ichi Hanai^{d,e}, Jovana Kaludjerovic^a, Michael J. Densmore^a, Quan Yuan^a, Hakan R. Toka^{e,2}, Martin R. Pollak^e, Jianghui Hou^f, and Beate Lanske^{a,b,3}

^aDivision of Bone and Mineral Research, Oral Medicine, Infection and Immunity, Harvard School of Dental Medicine, Boston, MA 02115; ^bEndocrine Unit, Massachusetts General Hospital and Harvard Medical School, Boston, MA 02114; ^cFaculté de Médecine, Paris Descartes University, INSERM U1151-CNRS UMR8253, 75006 Paris, France; ^dDivision of Interdisciplinary Medicine and Biotechnology, Department of Medicine, Beth Israel Deaconess Medical Center and Harvard Medical School, Boston, MA 02115; ^eDivision of Nephrology, Department of Medicine, Beth Israel Deaconess Medical Center and Harvard Medical School, Boston, MA 02115; and ^fDepartment of Internal Medicine, Washington University Renal Division, Washington University, St. Louis, MO 63130

Edited by John T. Potts, Massachusetts General Hospital, Charlestown, MA, and approved March 3, 2017 (received for review October 8, 2016)

Renal Ca^{2+} reabsorption is essential for maintaining systemic Ca^{2+} homeostasis and is tightly regulated through the parathyroid hormone (PTH)/PTHrP receptor (PTH1R) signaling pathway. We investigated the role of PTH1R in the kidney by generating a mouse model with targeted deletion of PTH1R in the thick ascending limb of Henle (TAL) and in distal convoluted tubules (DCTs): *Ksp-cre;Pth1r^{fl/fl}*. Mutant mice exhibited hypercalciuria and had lower serum calcium and markedly increased serum PTH levels. Unexpectedly, proteins involved in transcellular Ca^{2+} reabsorption in DCTs were not decreased. However, claudin14 (*Cldn14*), an inhibitory factor of the paracellular Ca^{2+} transport in the TAL, was significantly increased. Analyses by flow cytometry as well as the use of *Cldn14-lacZ* knock-in reporter mice confirmed increased *Cldn14* expression and promoter activity in the TAL of *Ksp-cre;Pth1r^{fl/fl}* mice. Moreover, PTH treatment of HEK293 cells stably transfected with CLDN14-GFP, together with PTH1R, induced cytosolic translocation of CLDN14 from the tight junction. Furthermore, mice with high serum PTH levels, regardless of high or low serum calcium, demonstrated that PTH/PTH1R signaling exerts a suppressive effect on *Cldn14*. We therefore conclude that PTH1R signaling directly and indirectly regulates the paracellular Ca^{2+} transport pathway by modulating *Cldn14* expression in the TAL. Finally, systemic deletion of *Cldn14* completely rescued the hypercalciuric and lower serum calcium phenotype in *Ksp-cre;Pth1r^{fl/fl}* mice, emphasizing the importance of PTH in inhibiting *Cldn14*. Consequently, suppressing CLDN14 could provide a potential treatment to correct urinary Ca^{2+} loss, particularly in patients with hypoparathyroidism.

PTH1R | CLDN14 | mouse kidney | hypercalciuria | paracellular

Renal calcium reabsorption is critical for maintaining systemic calcium homeostasis, and thus a failure in this process has severe health consequences (1). Renal calcium leak is widely recognized as the most common metabolic abnormality in calcium stone formers (2, 3), and it is also known to increase the risk of osteoporosis and fractures (4–6). However, the mechanisms of renal calcium reabsorption, and, consequently, the pathogenesis of renal calcium leak, are not completely understood. For this reason, treatments to reduce urinary Ca^{2+} excretion are still limited to dietary recommendations and thiazide diuretics (2, 3).

Sixty-five percent of renal calcium reabsorption takes place in the proximal tubules (PTs) through a paracellular solvent-drag, nonregulated pathway, and 25% occurs in the thick ascending limb of Henle (TAL) through a regulated paracellular pathway. The remaining 10–15% of calcium reabsorption takes place in the distal convoluted tubules (DCTs) via active transcellular transport. In the TAL, the apical $\text{Na}^+\text{-K}^+\text{-2Cl}^-$ cotransporter and renal outer medullary K^+ channel generate a lumen-positive transepithelial potential difference that drives calcium reabsorption via the paracellular pathway (7, 8). This process is controlled by specific tight-

junction molecules belonging to the claudin family. Claudins are tetraspan proteins that form paracellular channels allowing selective permeation of ions through the epithelial tight junction. Claudin-16 (CLDN16) and CLDN19 assemble a heteromeric paracellular complex constituting either an intercellular pore or an ion concentration sensor to regulate paracellular reabsorption of cations in the TAL. Previously, CLDN14, which is mainly expressed in the TAL, was found to bind to CLDN16 and to inhibit its channel permeability (9). CLDN14 thus acts as a negative gatekeeper for the heteromeric CLDN16/CLDN19 complex and modulates Ca^{2+} reabsorption in the TAL, likely in response to dietary Ca^{2+} load (8). Although it is well known that mutations in human genes encoding CLDN16 and CLDN19 are responsible for familial hypomagnesemia with hypercalciuria and nephrocalcinosis (Online Mendelian Inheritance in Man 248250) (10, 11), knowledge of the central role for CLDN14 in regulating renal paracellular calcium reabsorption emerged only few years ago. The key role of CLDN14 is supported by the striking observation that mice with global deletion of *claudin14* (*Cldn14^{-/-}*) show a failure in increase of urinary Ca^{2+} excretion in response to a high-calcium diet (9). In humans, a homozygous mutation in the *CLDN14* gene on chromosome 21q22 causes autosomal recessive nonsyndromic deafness-29 (12). More recently, *CLDN14* polymorphisms have

Significance

Renal calcium reabsorption is a critical process for maintaining systemic calcium homeostasis. Although the role of parathyroid hormone (PTH) in the regulation of transcellular Ca^{2+} reabsorption in distal convoluted tubules is well understood, its potential role in controlling the paracellular Ca^{2+} transport in the thick ascending limb of Henle (TAL) has not been investigated. We now present data demonstrating that PTH/PTHrP receptor (PTH1R) signaling directly and indirectly controls the levels of Claudin14 (CLDN14), a tight-junction protein responsible for paracellular Ca^{2+} transport in the TAL. Our findings suggest that down-regulation of Claudin14 could provide a potential treatment option to correct urinary Ca^{2+} loss, particularly in patients with hypoparathyroidism.

Author contributions: T.S. and B.L. designed research; T.S., N.I., Y.F., J. Hanai, J.K., and Q.Y. performed research; T.S., J. Hanai, H.R.T., M.R.P., and J. Hou analyzed data; and T.S., M.C., M.J.D., and B.L. wrote the paper.

The authors declare no conflict of interest.

This article is a PNAS Direct Submission.

¹M.C. and N.I. contributed equally to this work.

²Present address: Graduate Medical Education, Manatee Memorial Hospital, Bradenton, FL 34208.

³To whom correspondence should be addressed. Email: beate_lanske@hshdm.harvard.edu.

This article contains supporting information online at www.pnas.org/lookup/suppl/doi:10.1073/pnas.1616733114/-DCSupplemental.

also been associated with nephrolithiasis and low bone density, inferring a role for CLDN14 in the pathogenesis of renal calcium leak (13, 14).

Systemic calcium homeostasis is maintained by a well-coordinated regulation of renal calcium reabsorption; intestinal calcium absorption; and bone resorption by parathyroid hormone (PTH), 1,25(OH)₂D, and extracellular calcium itself via the calcium-sensing receptor (CaSR). PTH is secreted by the parathyroid glands in response to low serum calcium and vitamin D levels, and it stimulates calcium reabsorption, phosphate excretion, and the production of 1,25(OH)₂D in the kidney and can also induce bone resorption to stimulate the release of calcium and phosphate from the skeleton (15). It binds to and activates the PTH/PTHrP receptor (PTH1R), a G protein-coupled receptor that is expressed in many tissues but has

its highest expression in kidney and bone (16). PTH1R activates the adenylyl cyclase (cAMP), IP₃, PKC, and Ca²⁺ signaling pathways (17). In the kidney, PTH regulates the expression and function of the transient receptor potential vanilloid 5 (TRPV5) and of Calbindin 28K, two important proteins responsible for transcellular Ca²⁺ transport in the DCTs. This process has been extensively studied and is well understood (7). However, a potential role for PTH signaling via the PTH1R in controlling the paracellular calcium transport in the TAL has not been investigated so far.

It has been shown that the CaSR is expressed in the TAL and that an acute inhibition of CaSR increases the permeability of the paracellular pathway to Ca²⁺, independent of PTH actions (18). More recently, it has been discovered that CaSR regulates paracellular Ca²⁺ transport by modulating the expression of

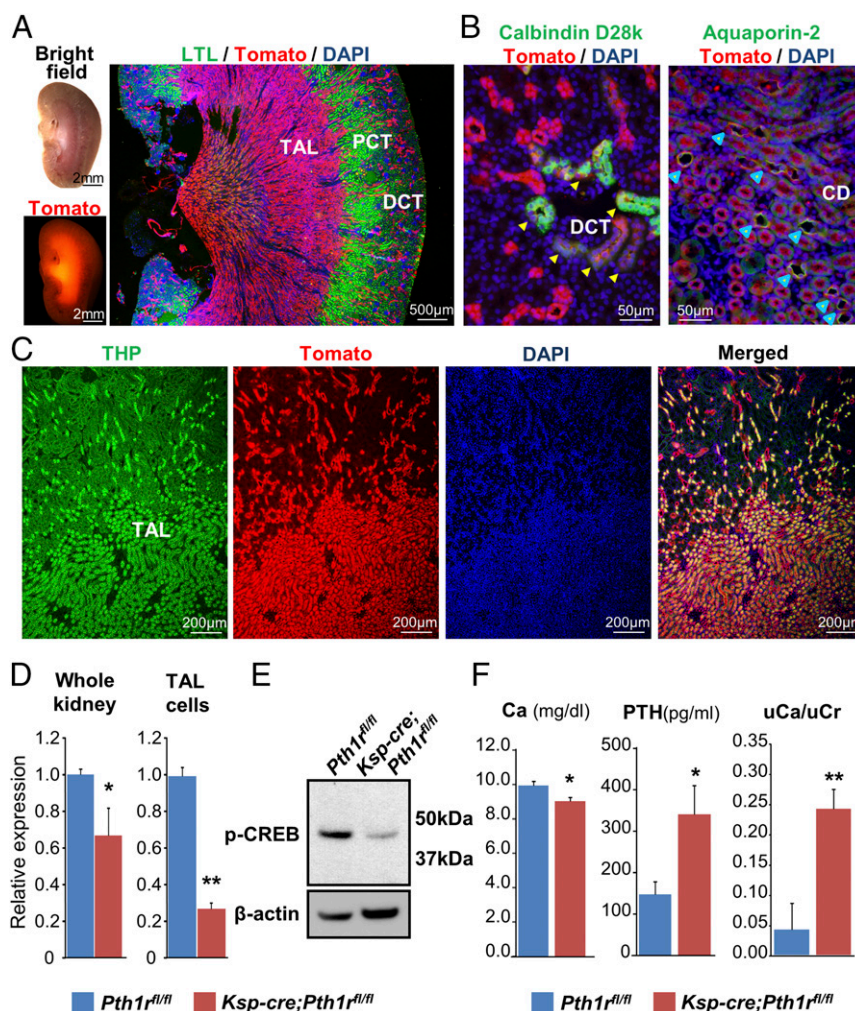


Fig. 1. Illustration of Ksp-cre specificity by immunofluorescence (IF) and analyses of renal tubule-specific deletion of *Pth1r*. (A, Left) Stereomicroscopic image of the whole kidney of a 6-wk-old *Ksp-cre;Tomato^{fl/+}* mouse visualized by bright-field and fluorescence for Tomato. (A, Right) Overview of a *Ksp-cre;Tomato^{fl/+}* kidney section by IF staining: blue (DAPI, nuclei), green [Lotus tetragonolobus Lectin (LTL)-specific staining for a proximal convoluted tubule (PCT)], and red (antibody staining for Tomato representing Cadherin-16/*Ksp-cre*-positive cells). No Tomato-positive staining was seen in glomeruli (blue nuclei, DAPI) and PCTs (green). (B) Higher magnification of kidney sections of *Ksp-cre;Tomato^{fl/+}* mouse triple-stained with various antibodies to determine the overlap of expression of Cadherin-16 (*Ksp-cre;Tomato*, red) with Calbindin D28k (green) in DCTs and DAPI (blue) (Left), and with Cadherin-16 (*Ksp-cre;Tomato*, red) with Aquaporin-2 (green) in CDs and DAPI (blue) (Right). Some Tomato-positive signals were found in DCTs and CDs, as shown by double staining with Calbindin D28k (yellow arrowheads) and Aquaporin-2, respectively. Aquaporin-2-positive cells (green) appear in yellow (turquoise arrowheads) due to the overlapping expression with *Ksp-cre;Tomato* (red). (C) Kidney section stained with antibodies for Tamm-Horsfall protein (THP, green) specific for the TAL, Tomato (red), and DAPI (blue). The merged image illustrates the strong overlap in expression of THP and *Ksp-cre;Tomato*, indicating that Cre activity is strongest in the TAL. (D) qRT-PCR analyses from whole-kidney (Left) and TAL (Right) RNA of 6-wk-old *Pth1r^{fl/fl}* and *Ksp-cre;Pth1r^{fl/fl}* mice confirms efficient deletion of *Pth1r* in mutants ($n = 5-10$). * $P < 0.05$; ** $P < 0.01$. (E) Expression of p-CREB protein, reflecting the PTH1R intracellular signaling pathway in the TAL from *Pth1r^{fl/fl}* and *Ksp-cre;Pth1r^{fl/fl}* mice, was determined by Western blot analysis, showing lower p-CREB levels in *Ksp-cre;Pth1r^{fl/fl}* mice compared with controls. (F) Serum and urinary (u) parameters of 6-wk-old *Pth1r^{fl/fl}* and *Ksp-cre;Pth1r^{fl/fl}* mice ($n = 5-6$). * $P < 0.05$; ** $P < 0.01$.

Cldn14 (19, 20). Expression of PTH1R has also been found in the TAL. However, due to its wide expression in the kidney, including the PT, TAL, and DCT (21), specific actions of PTH in modulating paracellular Ca^{2+} transport have not been identified. We therefore explored the role of PTH1R specifically in the distal parts of the nephron using a mouse model in which ablation of PTH1R was limited to the TAL, DCT, connecting tubule, and collecting duct (CD). Here, we report findings demonstrating that PTH1R signaling regulates paracellular Ca^{2+} transport by directly and indirectly modulating the expression of Cldn14 in the TAL.

Results

Generation and Characterization of *Ksp-cre;Pth1r^{fl/fl}* Mice. Mice with a specific *Pth1r* deletion in the distal parts of the nephron (TAL, DCT, connecting tubule, and CD) under the control of the *Ksp* promoter were generated using Cre-loxP recombination (Fig. S1 A and B). We first examined the in vivo expression pattern of Cadherin-16 Cre (*Ksp-cre*) mice using Tomato reporter mice (*Ksp-cre;Tomato^{fl/fl}*) (Fig. 1 A–C). Our analyses demonstrate that Cadherin-16 promoter-driven expression of tdTomato is primarily limited to the TALs and DCTs in the kidney, with a small amount of expression found in the CDs (Fig. 1 B and C). No expression was detected in the glomeruli or proximal convoluted tubules (Fig. 1A). We then confirmed efficient deletion of *Pth1r* in *Ksp-cre;Pth1r^{fl/fl}* mice by quantitative RT-PCR (qRT-PCR) using whole-kidney RNA, where we detected a statistically significant reduction in expression (~30%). We analyzed specific *Pth1r* deletion in the TAL by immune-isolating cells specific to the TAL with magnetic beads coupled to the Tamm–Horsfall protein antibody and observed a 75% reduction in *Pth1r* mRNA levels (Fig. 1D). The marked decrease in the phospho-CREB (p-CREB) band for the mutants (Fig. 1E) demonstrates the efficient reduction of PTH1R downstream signaling.

Macroscopic Phenotype and Analyses of Serum and Urinary Parameters. *Ksp-cre;Pth1r^{fl/fl}* mice appeared macroscopically normal in size and weight and were indistinguishable from their control littermates (Fig. S1 C and D). Serum and urine samples from 6-wk-old mice were collected for analyses of biochemical parameters. Interestingly, mutant mice showed significantly decreased serum calcium levels, markedly elevated serum PTH levels, and severe hypercalciuria (Fig. 1F). No major changes could be detected between *Pth1r^{fl/fl}* and *Ksp-cre;Pth1r^{fl/fl}* mice for serum phosphate (9.52 ± 0.49 vs. 9.74 ± 0.45 mg/dL, $n = 5$ –6), intact and C-terminal FGF23 levels (intact: 366 ± 57 vs. 429 ± 46 pg/mL, $n = 8$ –10; C-terminal: 715 ± 40 vs. 817 ± 77 pg/mL, $n = 14$ –15), urea nitrogen (34.5 ± 4.3 vs. 29.1 ± 4.0 mg/dL, $n = 7$), or creatinine (0.47 ± 0.09 vs. 0.28 ± 0.07 mg/dL, $n = 7$). Also, no differences in urinary nitrogen ($1,034 \pm 44$ vs. $1,038 \pm 110$ mg/dL, $n = 5$ –6) and urinary creatinine (22.0 ± 2.9 vs. 23.5 ± 5.4 mg/dL, $n = 5$ –6) could be detected. Moreover, renal gene expression of the vitamin D receptor (*Vdr*) and Klotho (*Kl*) was comparable between *Pth1r^{fl/fl}* and *Ksp-cre;Pth1r^{fl/fl}* mice (relative expression of *Vdr*: 1.00 ± 0.05 vs. 1.15 ± 0.04 , relative expression of *Kl*: 1.00 ± 0.00 vs. 0.94 ± 0.03). Gene expression was normalized to *Gapdh*. Moreover, no major changes in serum $1,25(\text{OH})_2\text{D}$ levels could be detected in *Ksp-cre;Pth1r^{fl/fl}* mice, which is in accordance with an unaltered expression of the 1α -hydroxylase and 24 -hydroxylase, despite higher serum PTH levels (Fig. S1E).

Expression of Genes Involved in Renal Calcium Transport. PTH1R signaling is critical for renal Ca^{2+} reabsorption in DCTs, so the significant increase in urinary Ca^{2+} was not unexpected. We then examined the expression of the well-known proteins responsible for transcellular Ca^{2+} transport in the DCTs: TRPV5 and Calbindin D28k. Surprisingly however, a significant increase in *Trpv5* and *calbindin D28k* mRNA and Calbindin D28k protein levels (Fig. 2 A and B) could be observed in *Ksp-cre;Pth1r^{fl/fl}*

mice, suggesting that the renal calcium leak cannot have occurred in that part of the kidney. This provocative finding led us to investigate further whether loss of PTH1R in the TAL could possibly affect paracellular permeation of calcium in the TAL. We compared the expression pattern of *Cldn14*, *Cldn16*, and *Cldn19* in *Ksp-cre;Pth1r^{fl/fl}* and *Pth1r^{fl/fl}* mice at 6 wk of age. Notably, we observed a greater than fivefold increase in basal *Cldn14* mRNA expression in whole kidneys of mutants compared with *Pth1r^{fl/fl}* littermates. Isolation of TAL-specific cells from control and mutant mice resulted in even higher expression levels of *Cldn14*. No apparent changes were found in *Cldn16* or *Cldn19* mRNA levels in either whole-kidney or TAL cells (Fig. 2C). Western blot analyses confirmed an increase in Cldn14 protein expression in isolated TAL cells of *Ksp-cre;Pth1r^{fl/fl}* mice and showed a slight decrease in Cldn16 and Cldn19 levels, suggesting that Cldn14 might control the Cldn16/Cldn19 complex (Fig. 2D).

We were able to support our data further by showing an increase in Cldn14 expression in *Ksp-cre;Pth1r^{fl/fl}* mice using flow cytometry of isolated TAL cells from *Ksp-cre;Tomato^{fl/+};Pth1r^{+/+}* control mice and *Ksp-cre;Tomato^{fl/+};Pth1r^{fl/fl}* mutant mice (Fig. 2E). Moreover, we could demonstrate enhanced *Cldn14* promoter activity in vivo by crossing control and mutant mice into the *Cldn14-lacZ* knock-in reporter mouse line, providing additional evidence by visualizing increased lacZ activity in renal tubules of *Ksp-cre;Pth1r^{fl/fl}* mice (Fig. 2F).

Effects of PTH and High Serum Calcium Levels on Claudin14 Expression.

We next tested the effects of PTH in the presence of high serum calcium levels on *Cldn14* expression by injecting 6-wk-old *Pth1r^{fl/fl}* and *Ksp-cre;Pth1r^{fl/fl}* mice with either vehicle (0.9% NaCl) or PTH (1–34) (50 nmol/kg of body weight). Serum and kidney samples were collected 2 h after treatment. As expected, PTH injection resulted in similar significant rises in serum calcium and $1,25(\text{OH})_2\text{D}$ levels in both genotypes. We also confirmed a marked increase in the expression of the 1α -hydroxylase, a well-known target gene of PTH, in the proximal convoluted tubules (PCTs) of both genotypes. This increased expression indicated a proper response to PTH and an intact function of PTH1R in portions of the kidney that are not affected by Cadherin-16 cre recombinase (Fig. 3A).

Consistent with our previous findings, *Cldn14* mRNA expression was markedly elevated (greater than fivefold) in mutant kidneys after vehicle (0.9% NaCl) injection compared with controls (Fig. 3B). PTH (1–34) injections did not affect *Cldn14* mRNA levels in *Pth1r^{fl/fl}* mice but did lead to a substantial up-regulation (>25-fold) of *Cldn14* expression in *Ksp-cre;Pth1r^{fl/fl}* without PTH1R in the TAL (Fig. 3B). These results suggest a regulatory mechanism in which an induction of *Cldn14* by high serum calcium is neutralized by suppression of *Cldn14* by PTH, as observed in *Pth1r^{fl/fl}* mice. However, in *Ksp-cre;Pth1r^{fl/fl}* mice, where the suppressive functions of PTH are absent, high serum calcium can freely stimulate *Cldn14* expression, resulting in markedly elevated Cldn14 levels.

Effects of Low Serum Calcium and High PTH Levels on Claudin14 Expression.

We and others have found that Cldn14 is positively correlated with dietary Ca^{2+} in that increased serum calcium levels lead to higher Cldn14 expression to promote Ca^{2+} excretion (9). On the other hand, reduced serum calcium levels result in suppression of Cldn14 to facilitate renal Ca^{2+} reabsorption (22). To determine whether deletion of PTH1R from the TAL disturbs this correlation, we challenged *Pth1r^{fl/fl}* and *Ksp-cre;Pth1r^{fl/fl}* mice by feeding them a Ca^{2+} -deficient diet. Immediately after weaning, mice were fed either a 0% Ca or 0.6% Ca control diet for a period of 3 wk, and were then killed and analyzed at 6 wk of age. As expected, serum calcium levels were significantly reduced in both mouse lines when fed the Ca^{2+} -deficient diet (Fig. 4A). This reduction in serum calcium levels was accompanied by high serum PTH (*Pth1r^{fl/fl}*: $1,675 \pm 221$ pg/mL and *Ksp-cre;Pth1r^{fl/fl}*: $1,729 \pm 183$ pg/mL, $n = 9$) and $1,25(\text{OH})_2\text{D}$ levels.

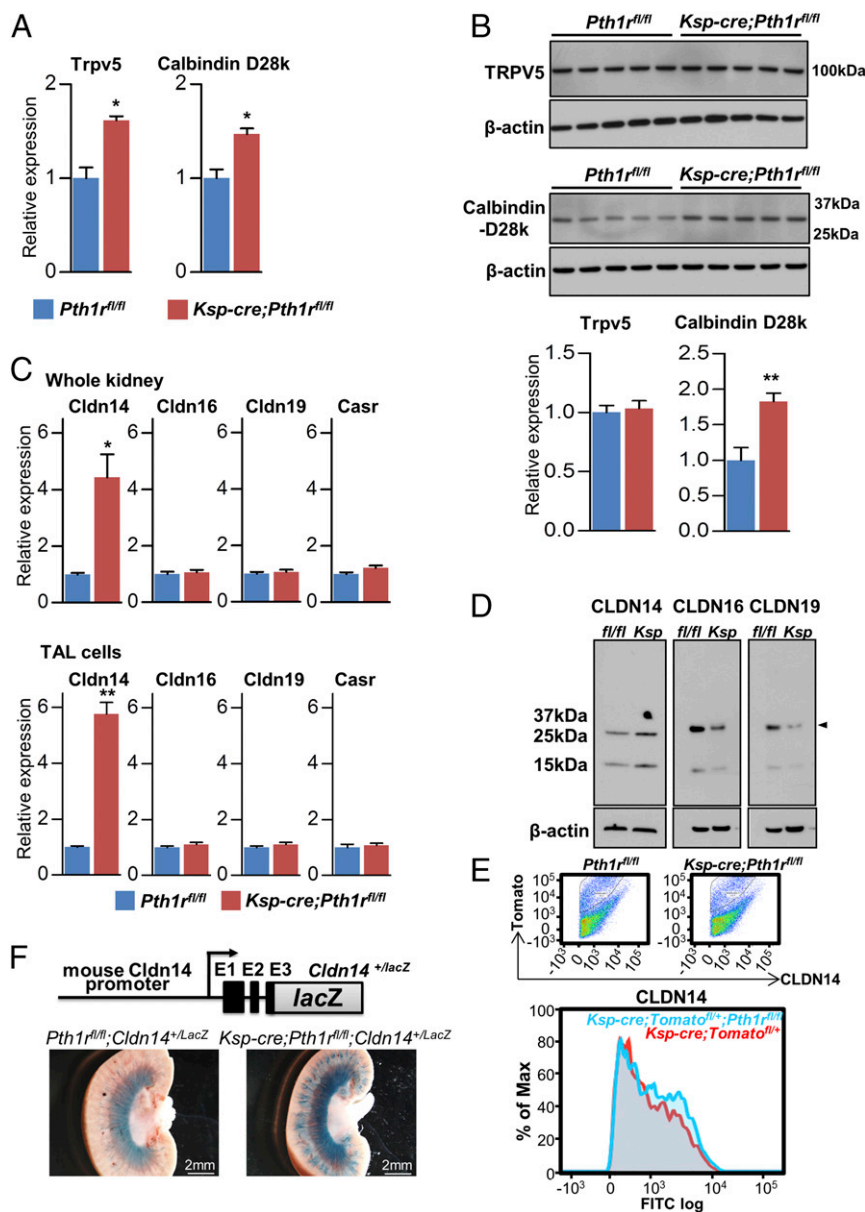


Fig. 2. Renal calcium transport proteins and gene expression. (A) mRNA expression of transcellular calcium transport proteins (Trpv5, Calbindin D28k) in whole kidneys of *Pth1r^{fl/fl}* and *Ksp-cre;Pth1r^{fl/fl}* mice at 6 wk of age ($n = 3-4$). Gene expression was normalized to *Gapdh*. * $P < 0.05$. (B) Protein expression of TRPV5 and Calbindin D28k. The protein expression was quantified by image-analyzing software (ImageJ) and normalized to β -actin. Calbindin D28k was up-regulated in *Ksp-cre;Pth1r^{fl/fl}* mice compared with the control group ($n = 5$). ** $P < 0.01$. (C) mRNA expression of paracellular calcium transport proteins (*Cldn14*, *Cldn16*, and *Cldn19*) and *Casr* in whole kidneys of *Pth1r^{fl/fl}* and *Ksp-cre;Pth1r^{fl/fl}* mice at 6 wk of age ($n = 3-4$). *Cldn14* expression in isolated TAL cells from *Ksp-cre;Pth1r^{fl/fl}* mice was markedly up-regulated. Gene expression was normalized to *Gapdh*. * $P < 0.05$; ** $P < 0.01$. (D) Protein expression of Cldn14, Cldn16, and Cldn19. Cldn14 expression (25.7 kDa) in *Ksp-cre;Pth1r^{fl/fl}* mice was up-regulated, whereas Cldn16 (~26 kDa) and Cldn19 (~26 kDa) were down-regulated. The black arrow depicts the expected band size for Cldn14, Cldn16, and Cldn19. The 10- to 15-Da band is common to all claudins and might represent a cleaved fragment. (E) Flow cytometry of Cldn14 in the TAL. Renal cells expressing Tomato protein were isolated from *Ksp-cre;Tomato^{fl/+};Pth1r^{fl/+}* and *Ksp-cre;Tomato^{fl/+};Pth1r^{fl/fl}* mice. Cldn14 expression was assessed in Tomato-positive cells from whole kidneys from mutant and control mice. Max, maximum. (F) In vivo *Cldn14* promoter-LacZ reporter assay. LacZ staining was performed in kidneys from *Pth1r^{fl/fl};Cldn14^{+/lacZ}* mice and *Ksp-cre;Pth1r^{fl/fl};Cldn14^{+/lacZ}* mice, showing increased LacZ staining in *Ksp-cre;Pth1r^{fl/fl};Cldn14^{+/lacZ}* kidneys.

Importantly, *Cldn14* mRNA expression in *Pth1r^{fl/fl}* mice was fully suppressed in response to both (i) the low serum calcium, and (ii) the high serum PTH levels compared with mice fed the control diet (Fig. 4B). In contrast, *Cldn14* expression in *Ksp-cre;Pth1r^{fl/fl}* mice fed a Ca^{2+} -deficient diet remained relatively high, and levels were comparable to the ones seen in control mice on the regular 0.6% calcium diet (Fig. 4B). Although *Cldn14* expression in *Ksp-cre;Pth1r^{fl/fl}* mice was markedly reduced in response to low serum calcium, we believe that the remaining

Cldn14 levels are due to the failure of PTH to suppress them in the absence of the PTH1R in the TAL. The failure in full suppression of *Cldn14* in kidneys of *Ksp-cre;Pth1r^{fl/fl}* mice implies that PTH can regulate *Cldn14* expression independent of serum calcium levels. We also generated *Casr^{-/-}* mice (22) as an alternative to feeding a Ca^{2+} -deficient diet. These mice cannot sense calcium, and therefore fail to induce *Cldn14*. In addition, *Casr^{-/-}* mice have high serum PTH levels, which further suppress *Cldn14*, resulting in total loss of *Cldn14* expression (Fig. S2 A

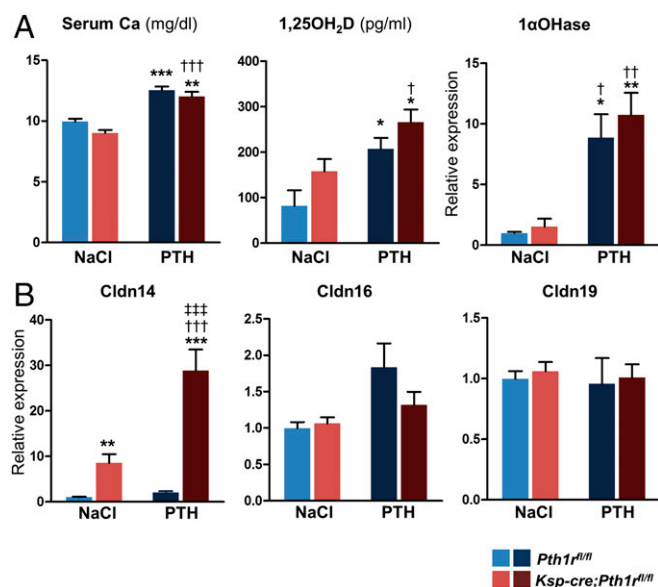


Fig. 3. PTH (1–34) injection into *Pth1r^{fl/fl}* and *Ksp-Cre;Pth1r^{fl/fl}* mice. (A) Serum Ca and 1,25(OH)₂D₃ and 1αOHase mRNA expression in 6-wk-old *Ksp-cre;Pth1r^{fl/fl}* and *Pth1r^{fl/fl}* mice ($n = 5–6$) 2 h after injection of 0.9% NaCl (vehicle) or PTH (1–34). (B) mRNA expression of *Cldn14*, *Cldn16*, and *Cldn19* in kidneys of *Pth1r^{fl/fl}* and *Ksp-cre;Pth1r^{fl/fl}* mice at 6 wk of age ($n = 3–4$) 2 h after injection of 0.9% NaCl or PTH (1–34). Expression was normalized to *Gapdh*. * $P < 0.05$, ** $P < 0.01$, *** $P < 0.001$ vs. NaCl in *Pth1r^{fl/fl}*; † $P < 0.05$; †† $P < 0.01$, ††† $P < 0.001$ vs. NaCl in *Ksp-cre;Pth1r^{fl/fl}*; †††† $P < 0.001$ vs. PTH in *Pth1r^{fl/fl}*.

and B) accompanied by a marked reduction in urinary Ca²⁺ excretion (Fig. S2B) to preserve calcium. No significant changes in expression of *Cldn16/19* were detected in any of these models (Fig. S2A). Moreover, *Trpv5* and *calbindin D28k* levels were largely unaltered upon low-calcium challenge, except for some increase in *calbindin D28k* in *Ksp-cre;Pth1r^{fl/fl}* mice, which could be explained as a compensatory attempt to recover some calcium that was lost in the TAL due to the remaining presence of *Cldn14* (Fig. S3).

PTH Modulates Cldn14 Membrane Expression. We then investigated potential direct effects of PTH on claudin proteins by stably transfecting CLDN14-GFP, CLDN16-GFP, and CLDN19-GFP fusion proteins in HEK293 cells that also express human PTH1R. It has previously been reported that the tight-junction inhibitor sodium decanoate (C10) can alter the distribution of claudins, and thereby suppress the tight-junction barrier function (23, 24). To test our cell system, we performed fluorescence analysis over a 2- to 3-h period and confirmed that C10 treatment immediately relieves the tight junction between cells and increases CLDN14 protein expression on the cell–cell junctions (Fig. S4). Subsequently, we tested the effects of PTH (1–34) on CLDN proteins in each of these cell lines. Time-lapse microscopy shows that PTH induces translocation of CLDN14, whereby the protein moves from discrete nodules on the cell membrane to a more even distribution along the cell membrane and also to the cytosol. PTH had no observable effect on CLDN16 or CLDN19 in this assay (Fig. 5A). We further investigated the CLDN14 nodular structures on the cell–cell junction by generating 3D reconstruction images with serial z-stack optical sections. Fig. 5B (Left) shows 3D reconstitution images of CLDN14, CLDN16, and CLDN19 before and after 180 min of PTH treatment. Fig. 5B (Right) represents the quantification, with red and yellow colors indicating higher expression of CLDNs located on tight junctions and blue-shaded colors representing relatively lower claudin expression in the cytosol. Our results indicate that PTH treatment significantly altered the

distribution of CLDN14 from thick nodular structures, presumably tight junctions, to a more diffuse, thin-lined structure and more CLDN14 signal in the cytosol (light blue in Fig. 5B, Right).

Increased Claudin14 Expression in *Ksp-cre;Pth1r^{fl/fl}* Mice Is Responsible for the Hypercalciuria. We now examined whether the hypercalciuria observed in *Ksp-cre;Pth1r^{fl/fl}* mice is due to the increased *Cldn14* levels. We crossed the *Ksp-cre;Pth1r^{fl/fl}* mice into the global *Cldn14^{-/-}* background (*Cldn14^{-/-};Ksp-cre;Pth1r^{fl/fl}*). *Cldn14* expression is limited to the inner ear and the TAL of the kidney, so loss of its function was not expected to result in any gross developmental defects. *Cldn14^{-/-}* mice challenged with a high-Ca²⁺ diet have previously been shown to preserve calcium inadequately (9), so we anticipated that loss of its function in *Ksp-cre;Pth1r^{fl/fl}* mice could rescue the observed calcium leak. We first confirmed the complete absence of *Cldn14* in our double-mutant mouse models (*Cldn14^{-/-};Pth1r^{fl/fl}* and *Cldn14^{-/-};Ksp-cre;Pth1r^{fl/fl}*) as demonstrated by the undetectable mRNA levels in the kidney of these mice (Fig. 6A) compared with controls (*Pth1r^{fl/fl}* and *Ksp-cre;Pth1r^{fl/fl}* mice). We then collected serum and urine, and measured urinary Ca²⁺ excretion in all four genotypes. As anticipated, deletion of *Cldn14* from *Ksp-cre;Pth1r^{fl/fl}* mice was able to prevent the urinary Ca²⁺ loss and restore levels comparable to the ones seen in control mice (Fig. 6B). This finding provides evidence that the hypercalciuria in *Ksp-cre;Pth1r^{fl/fl}* mice is primarily due to elevated *Cldn14* expression and that PTH1R signaling in the TAL is critical to suppress *Cldn14*. The elimination of the calcium leak also corrected the lower serum calcium and higher PTH levels in *Cldn14^{-/-};Ksp-cre;Pth1r^{fl/fl}* mice (Fig. 6C).

Discussion

Maintenance of systemic calcium homeostasis is crucial and requires a constant regulation of various proteins involved in calcium sensing, intestinal Ca²⁺ absorption, renal Ca²⁺ reabsorption, and bone resorption. PTH is a well-established endocrine hormone involved in these processes, and any alterations in its own activity or in the function of its receptor, PTH1R, can lead to mineral disorders (25–27). In this study, we demonstrate that loss of PTH1R specifically in the distal parts of the nephron results in hypercalciuria and slightly lower serum calcium levels in *Ksp-cre;Pth1r^{fl/fl}* mice compared with control littermates. *Pth1r^{fl/fl}* and *Ksp-cre;Pth1r^{fl/fl}* mice had similar creatinine levels, indicating that the glomerular filtration rate was also similar. Taken together, the stable serum creatinine levels and the slight decrease in serum calcium in *Ksp-cre;Pth1r^{fl/fl}* mice suggest that the observed urinary Ca²⁺ leak is due to decreased renal calcium reabsorption rather than increased filtered calcium load. The calcium imbalance explains the elevated serum PTH levels in the mutant mice.

PTH has been shown to enhance transcellular renal Ca²⁺ reabsorption by stimulating the expression of TRPV5 and Calbindin D28k (28, 29). Importantly, the higher activity and prolonged presence of TRPV5 at the apical membrane enhance calcium reabsorption in the DCT (29, 30). Although there is no doubt that PTH can regulate TRPV5, most of the experiments were performed more than 7 y ago and the findings are predominantly based on in vitro experiments using cell cultures (29–32). In our study using an in vivo model, *Ksp-cre;Pth1r^{fl/fl}* mice did not show the anticipated decline in levels of *Trpv5* and *calbindin D28k*, but rather presented with elevated mRNA and/or protein levels. Although we did not directly measure Ca²⁺ transport in the different segments of the tubule, these findings suggest that the observed urinary Ca²⁺ loss is not primarily due to a failure in transcellular calcium transport in the DCT and imply that PTH might exert additional regulatory functions in other segments of the kidney, such as the TAL. In fact, we could demonstrate a significant increase in *Cldn14* mRNA and protein expression associated with tight junctions in the TAL upon loss

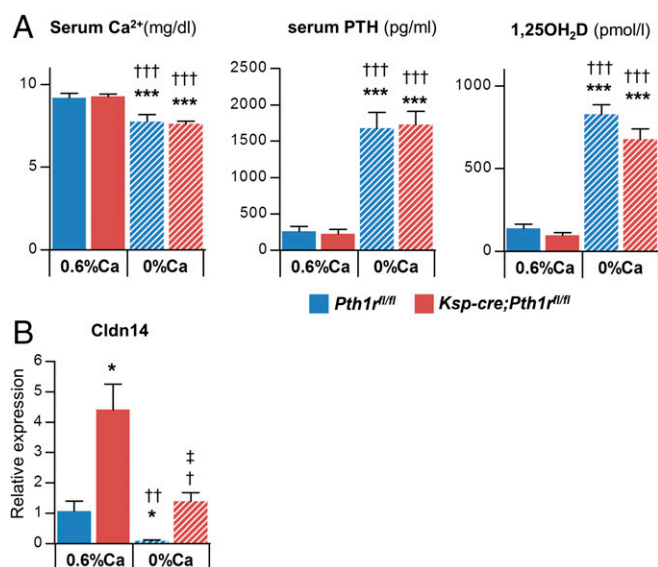


Fig. 4. *Ksp-cre;Pth1r^{fl/fl}* mice on a Ca-deficient diet. Mice were fed either a control Ca²⁺ (0.6% Ca) or Ca²⁺-deficient (0% Ca) diet for 3 wk. (A) Serum calcium, PTH, and 1,25(OH)₂D of 6-wk-old *Pth1r^{fl/fl}* and *Ksp-cre;Pth1r^{fl/fl}* mice ($n = 5-6$). *** $P < 0.001$ vs. *Pth1r^{fl/fl}* on 0.6% Ca; ††† $P < 0.001$ vs. *Ksp-cre;Pth1r^{fl/fl}* on 0.6% Ca. (B) mRNA expression of the paracellular Ca²⁺ transport protein *Cldn14* in *Pth1r^{fl/fl}* and *Ksp-cre;Pth1r^{fl/fl}* mice on the control diet and Ca²⁺-deficient diet. * $P < 0.05$ vs. *Pth1r^{fl/fl}* on 0.6% Ca²⁺; † $P < 0.05$, †† $P < 0.01$ vs. *Ksp-cre;Pth1r^{fl/fl}* on 0.6% Ca²⁺; † $P < 0.05$, †† $P < 0.01$ vs. *Pth1r^{fl/fl}* on 0% Ca²⁺.

of PTH1R. This finding is consistent with the presence of a CREB response element in the mouse *Cldn14* promoter, located between -100 and -111 bp (chromosome 16: 94008935-94008946) from the transcriptional start site (NM_019500, <https://genome.ucsc.edu/>). CLDN14 has been described to act as a negative gatekeeper for the heteromeric CLDN16/CLDN19 complex to modulate Ca²⁺ reabsorption in the TAL; thus, an increase in CLDN14 would be expected to result in renal calcium leak. Also, polymorphisms in human CLDN14 have recently been associated with nephrolithiasis (13, 14), and global *Cldn14*^{-/-} mice fail to excrete urinary Ca²⁺ efficiently when needed (9). We therefore believe that the slight increase in *Trpv5* and *calbindin 28K* could reflect a compensatory mechanism as an attempt to preserve calcium in DCTs that was lost in the TAL of *Ksp-cre;Pth1r^{fl/fl}* mice. Such a process could be initiated by the high urinary Ca²⁺ load that is sensed by either the conventional CaSR pathway or another calcium sensor expressed at the apical membrane of the DCT cells (33, 34). Another explanation could be that the transcellular calcium transport in the DCTs is stimulated by the slightly increased serum calcitriol levels (35). Of course, we cannot exclude the possibility that some PTH1R-positive cells are still expressed in DCTs, and could therefore mediate these actions. If such is the case, however, the small remaining amount of PTH1R is not sufficient to compensate fully for the renal calcium leak.

We also discovered a direct posttranslational effect of PTH on CLDN14 by developing a cell culture model with cells coexpressing PTH1R and CLDN14. We found that PTH treatment disrupted the proper, patchy membranous expression of CLDN14 and induced cytosolic translocation. Interestingly, PTH did not alter the membranous expression pattern of CLDN16 or CLDN19 in corresponding cell lines. These findings are consistent with posttranslational regulation of CLDN14 by PTH1R signaling without directly affecting CLDN16 or CLDN19. The reduced *Cldn16* and *Cldn19* protein levels observed in *Ksp-cre;Pth1r^{fl/fl}* mice are likely an indirect effect resulting from the high *Cldn14* levels in these mice. One possible mechanism for CLDN14 posttranslational regulation by PTH is the

phosphorylation of CLDN14 and/or PDZ proteins [e.g., zonula occludens-1 (ZO-1), ZO-3], which can bind to CLDN14. This hypothesis is consistent with previous studies reporting that the serine 217 in the carboxyl terminus of CLDN16 was phosphorylated by PKA to regulate the CLDN16-ZO-1 (tight-junction molecule-ZO-1) interaction required to maintain the tight junction (36). Other protein modifications initiated by PTH1R signaling could be responsible as well. It has been reported that CLDN14 delocalization was related to mutation of membrane-proximal cysteines in the second and fourth transmembrane domains, which are possible palmitoylation sites. However, the palmitoylation mutant CLDN14 remained concentrated at sites of cell-cell contact and was competent to assemble into freeze-fracture strands when expressed in fibroblasts (37). This result suggests that CLDN14 palmitoylation is important for efficient localization into tight junctions but not for stability or strand assembly. Because we observed that PTH treatment decreased CLDN14 on the cell-cell junction and induced its cytosolic translocation, PTH might directly modulate CLDN14 modification sites (e.g., palmitoylation) in the stable cell line, and this action could contribute to the regulation of renal Ca²⁺ reabsorption in vivo. However, further experiments are needed to identify the mechanisms responsible for the posttranslational regulation of CLDN14 by PTH definitively and to determine potential CLDN14 binding partners associated with PTH1R signaling. Taken together, our in vivo and in vitro data demonstrate that PTH modulates CLDN14 levels and subcellular localization through transcriptional and posttranslational mechanisms, highlighting that CLDN14 is a key target for PTH to maintain proper renal Ca²⁺ reabsorption in the TAL.

Research has shown that *Cldn14* is regulated by calcium via the CaSR expressed in the TAL (19, 20, 22). We have confirmed that loss of CaSR in mice results in decreased expression of *Cldn14*, in turn, resulting in decreased urinary Ca²⁺ excretion (Fig. S2). This finding provides additional evidence that low serum calcium levels reduce *Cldn14* and thereby promote renal Ca²⁺ reabsorption. PTH is the major regulator of systemic calcium homeostasis, so we explored whether PTH regulates *Cldn14* via a calcium-dependent mechanism only or whether PTH can affect *Cldn14* regardless of serum calcium levels. We analyzed the effects of high serum PTH in the presence of either high serum calcium (Fig. 3) or low serum calcium (Fig. 4) levels. First, we found that PTH (1-34) injection resulted in high serum calcium levels in control and mutant mice (Fig. 3). However, only mutant mice responded with a marked increase (>25-fold) in *Cldn14* expression. PTH1R is absent in these mice, so the elevation in *Cldn14* levels can only be explained by an induction by high serum calcium (Fig. 7D). Interestingly, *Pth1r^{fl/fl}* mice did not show any changes in *Cldn14*, indicating that the presence of the PTH1R in the TAL of control mice can neutralize the effects of high serum calcium by suppressing *Cldn14* levels (Fig. 7C).

Second, feeding mice a low-calcium diet resulted in comparable low serum calcium and high serum PTH levels in both *Pth1r^{fl/fl}* and *Ksp-cre;Pth1r^{fl/fl}* mice. It is important to note that *Cldn14* expression in control mice was completely abolished as expected (Fig. 7E). In contrast, the very high basal *Cldn14* levels in *Ksp-cre;Pth1r^{fl/fl}* mice were decreased, yet levels remained significantly higher and were similar to the ones found in control mice on a normal diet (Fig. 7F). These data infer that in control mice, both low serum calcium and high PTH inhibited *Cldn14* levels. The same result was also observed in *Casr^{-/-}* mice (Fig. S2A). *Ksp-cre;Pth1r^{fl/fl}* mice are resistant to PTH actions in the TAL, so only low serum calcium could effectively inhibit *Cldn14* expression. These findings provide firm evidence that PTH modulates the function of *Cldn14* regardless of serum calcium levels. We propose that this dual role of PTH provides a system to fine-tune renal calcium reabsorption in the TAL and that calcium reabsorption in DCTs adds another level of control to assure a tight regulation of renal calcium handling.

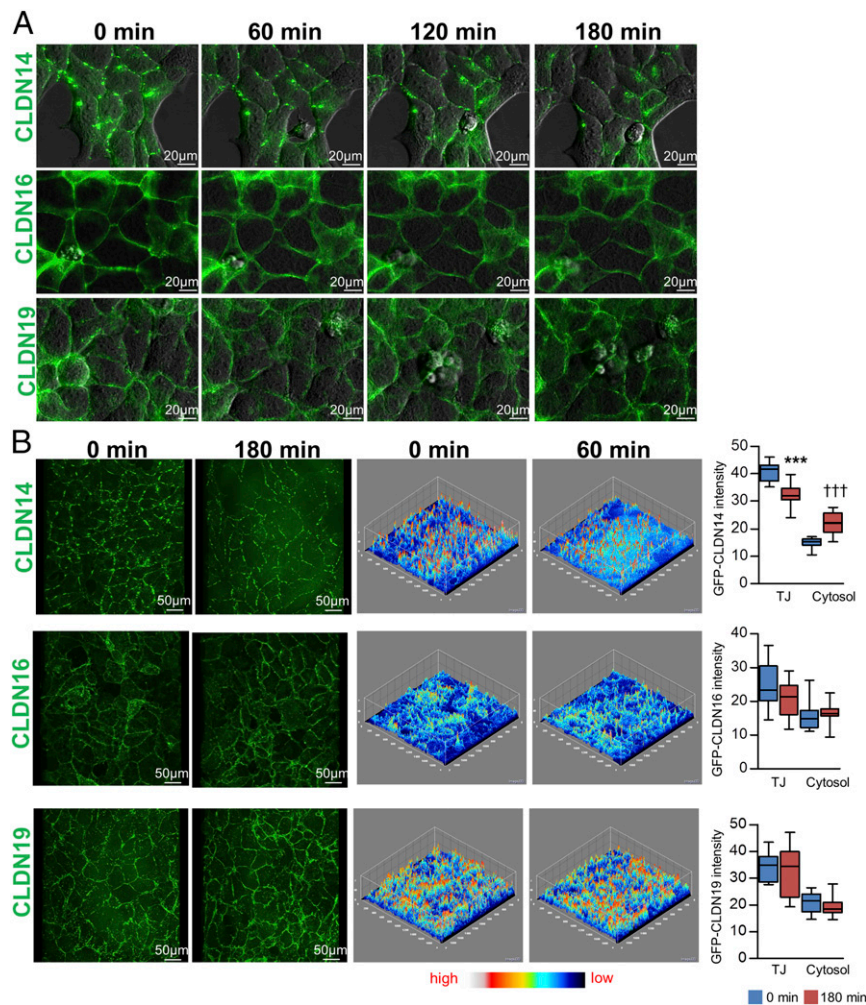


Fig. 5. In vitro analyses of translocation of paracellular Ca transport proteins upon PTH (1–34) treatment. (A) Localization of CLDN14-GFP, CLDN16-GFP, and CLDN19-GFP proteins is shown by IF in HEK293 cells stably overexpressing CLDN14 and PTH1R, CLDN16 and PTH1R, and CLDN19 and PTH1R at 0, 60, 120, and 180 min after PTH (1–34) treatment. Cells were placed on a 35-mm, no. 1.5 glass-bottomed culture dish for 2 d before imaging. Time-lapse microscopy was performed using a VivaView incubator fluorescence microscope. CLDN14-GFP is clearly visible as nodular structures on the cell–cell junction at 0 min. PTH treatment decomposed this structure over time into a weaker and more linear expression pattern along the cell membrane. No major changes were observed for CLDN16-GFP and CLDN19-GFP proteins. (B) Three-dimensional reconstruction images with serial z-stack optical sections. (Left) Three-dimensional reconstitution images of CLDN14, CLDN16, and CLDN19 before and after 180 min of PTH treatment. (Right) Quantification, with red and yellow colors indicating higher expression of claudins located on tight junctions and blue-shaded colors representing relatively lower claudin expression in the cytosol. PTH treatment significantly altered the distribution of CLDN14 from a thick nodular structure to a thin lined structure. The cytosolic CLDN14 diffuse pattern was increased by PTH treatment (light blue). The quantification is shown by box-and-whisker plots. PTH treatment significantly decreased tight-junction (TJ) CLDN14 and increased cytosolic CLDN14 ($n = 16$). $***P < 0.001$ vs. 0 min on tight junction; $+++P < 0.001$ vs. 0 min in cytosol.

Not only did we investigate the interaction of PTH and calcium levels in regulation claudin14 but we also looked for a potential role for vitamin D, which is an important regulator of calcium-reabsorbing proteins such as Trpv5 and Calbindin 28K (38). We observed that a Ca^{2+} -deficient diet resulted in lower *Cldn14* mRNA expression in the presence of lower serum calcium and higher serum $1,25(\text{OH})_2\text{D}$ levels. On the other hand, PTH injections induced high serum calcium and $1,25(\text{OH})_2\text{D}$ levels, but *Cldn14* mRNA expression remained unchanged. This observation clearly excludes active vitamin D as a regulator of *Cldn14* and strongly suggests that only the CaSR pathway, together with PTH, is responsible for the modulation of *Cldn14* expression (Fig. 7 A–F). The final proof for this hypothesis would be to generate mice with deletion of both *Casr* and *Pth1r* in renal tubules, which could be the focus of a follow-up study.

Finally, we could demonstrate that genetic deletion of *Cldn14* from *Ksp-cre;Pth1r^{fl/fl}* mice was able to rescue their hypercalcemic phenotype and normalize the slightly lower serum calcium levels.

This finding provides firm evidence that in the absence of PTH1R signaling in the TAL, the unregulated expression of *Cldn14* is responsible for the observed urinary Ca^{2+} loss. Therefore, PTH/PTH1R signaling plays a significant role in directly suppressing *Cldn14* to counterbalance the opposing and stimulating effects of calcium on *Cldn14* expression. We have shown that this dual function of PTH to (i) induce *Cldn14* expression via increasing serum calcium and (ii) suppress *Cldn14* regardless of serum calcium levels is critical to assure proper urinary Ca^{2+} reabsorption in the TAL.

In conclusion, our study demonstrates a function for PTH/PTH1R signaling in the regulation of paracellular calcium transport in the TAL. We provide compelling biological evidence that PTH1R signaling can directly and indirectly regulate *Cldn14*. We also demonstrate that CLDN14 is a direct target of PTH transcriptional and posttranslational regulation. Moreover, we show that PTH can indirectly modulate *Cldn14* via changing serum calcium levels via a

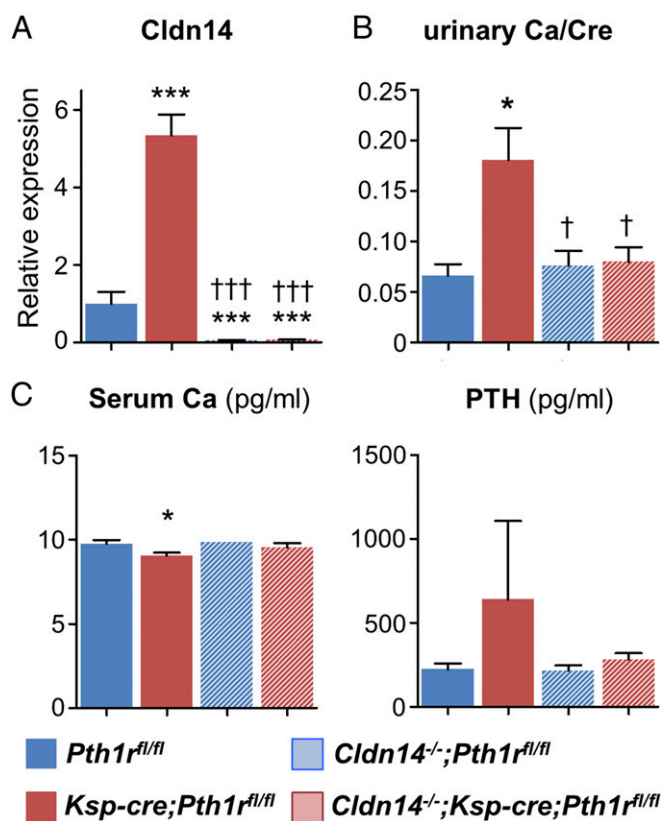


Fig. 6. Deletion of *Cldn14* from *Ksp-cre;Pth1r^{fl/fl}* mice fully rescues the urinary Ca^{2+} leak. Analyses of serum and urine parameters as well as renal mRNA expression of *Cldn14* in *Pth1r^{fl/fl}*, *Ksp-cre;Pth1r^{fl/fl}*, *Cldn14^{-/-};Pth1r^{fl/fl}*, and *Cldn14^{-/-};Ksp-cre;Pth1r^{fl/fl}* mice are shown. (A) Renal *Cldn14* mRNA expression in 6-wk-old mice shows complete absence of *Cldn14* in double mutants (striped bars in B and C). Urinary $Ca^{2+}/creatinine$ (B) and serum calcium and PTH (C) levels of 6-wk-old mice are shown ($n = 3-7$). * $P < 0.05$, *** $P < 0.001$ vs. *Pth1r^{fl/fl}*; † $P < 0.05$, ††† $P < 0.001$ vs. *Ksp-cre;Pth1r^{fl/fl}*.

CaSR-dependent pathway. A recent genome-wide association study of circulating PTH levels using 29,155 participants discovered five loci that were associated with variation in PTH levels. Notably, a robust association implicated *CLDN14*, the gene encoding *Claudin-14*. This finding further underscores the important connection between claudin-14 and PTH, even on a population level (39). Defects in *CLDN14* function have been implicated with hypercalciuria and nephrolithiasis (40). However, the regulation of this paracellular transport pathway has not been fully understood, hindering the development of therapies to correct calcium reabsorption abnormalities in diseases. Our findings suggest that *CLDN14* down-regulation could provide a potential treatment to correct urinary Ca^{2+} loss in humans, especially in the presence of low serum PTH levels as found in patients with hypoparathyroidism.

Materials and Methods

Animals. Mice with renal tubule-specific PTH1R deletion were generated using the Cre-loxP recombination system as previously described (41, 42). In brief, loxP sequences were introduced into the flanking regions of exon 1 of the *Pth1r* gene. Floxed mice were crossed with *Ksp-cre* transgenic mice [*B6.Cg-Tg(Cdh16-cre)91Igr/J*; The Jackson Laboratory] in which Cre recombinase expression is driven by the cadherin 16 promoter (Fig. S1A). Floxed littermates without Cre were used as wild-type controls. The in vivo expression pattern of Cre driven by the *Ksp* promoter was studied using Tomato reporter mice [*B6.Cg-Gt(ROSA)26Sortm14(CAG-tdTomato)Hze/J*, 007914; The Jackson Laboratory] crossed with *Ksp-cre* mice (*Ksp-cre;Tomato^{fl/+}*). *Cldn14*-deficient mice (*Cldn14^{-/-}*) mice were obtained from Tamar Ben-Yosef, Technion Israel Institute of Technology, Haifa, Israel and backcrossed to *C57BL/6* background

for seven generations (9). In the targeted allele, a lacZ cassette is expressed under the *Cldn14* promoter. Animals expressing Cre recombinase driven by the protamine 1 promoter [*129Sv-Tg(Prm-cre)58Og/J*] were obtained from The Jackson Laboratory. These mice were crossed with our conditional *Casr^{fl/+}* mice (22) to generate germline *Casr*-deficient (*Casr^{-/-}*) mice. Genotypes were determined by PCR and electrophoresis (Fig. S1B). Mice were fed a standard chow containing 0.81% calcium and 0.6% phosphorus (5058 LabDiet; Lab Supply). Low-calcium diet studies were performed using calcium-deficient and control diets. The calcium-deficient diet contained 0% calcium and 0.4% phosphorus based on American Institute of Nutrition, Research Diets (AIN-93). The control calcium diet contained 0.6% calcium and 0.4% phosphorus. Mice were fasted for 4 h before blood and urine collection. All studies performed were approved by the Institutional Animal Care and Use Committee of the Harvard Medical School.

Biochemical Analyses. Blood was obtained by cheek pouch puncture. Urine was gathered by spot collection using 1.7-mL polystyrene tubes. Total serum calcium and phosphorus levels as well as urinary Ca^{2+} , phosphorus, nitrogen, and creatinine levels were determined using Stanbio LiquiColor Kits (Stanbio Laboratory). Serum intact and C-terminal FGF23, PTH, and 1,25(OH) $_2$ D were measured by ELISA or enzyme immunoassay kits purchased from Immunotopics, Kainos Laboratories, and IDS. Urinary Ca^{2+} was normalized by creatinine.

TAL Cell Isolation. TAL cells were isolated by the immune magnetic separation method. Briefly, mouse renal tissues were dissected and treated with collagenase I in Ca^{2+} and Mg^{2+} concentration-adjusted Dulbecco's phosphate-buffered saline. After collagenase digestion, renal cells were washed and incubated with rabbit polyclonal anti-Tamm-Horsfall Glycoprotein (Bio-medical Technologies) that was coated on the paramagnetic polystyrene magnetic beads (Dynabeads M-280; DYNAL) to immunoprecipitate the TAL cells. The isolated cells were used for mRNA expression and Western blot analyses.

RNA Isolation and Transcript Analyses. Total RNA was collected from whole-kidney or renal TAL cells using TRIzol reagent (Life Technologies) according to the manufacturer's protocol. For qRT-PCR, cDNA was prepared using the QuantiTect Reverse Transcription Kit (Qiagen) and analyzed with Fast-Start Universal SYBR Green Master (ROX; Roche) in the StepOnePlus Real-Time PCR System (Applied Biosystems) using specific primers designed for each targeted gene. Relative expression was calculated using the $2^{-\Delta\Delta CT}$ method by normalizing with *Gapdh* housekeeping gene expression and presented as the fold increase relative to control.

Western Blotting. To test *Cldn14*, *Cldn16*, *Cldn19*, *Trpv5*, *Calbindin D28k*, and *p-CREB* expression in kidney and renal TAL cells, half of the kidney or isolated TAL cells were homogenized with radioimmunoprecipitation assay buffer (Alfa Aesar) with phosphatase and protease inhibitor mixture tablets (Roche) and centrifuged at $14,000 \times g$. The supernatant was then transferred to a fresh tube. Protein samples were heated with NuPAGE LDS Sample buffer (4x) (Life Technologies) and NuPAGE Reducing Agent (10x) (Life Technologies) at $70^\circ C$ for 10 min, and were then subjected to NuPAGE 4–12% Bis-Tris SDS/PAGE using precast gels (Invitrogen) and NuPAGE MES SDS running buffer (Life Technologies). The separated proteins were transferred to iBlot Gel Transfer Stacks PVDF (Life Technologies) via an iBlot Gel Transfer Device (Life Technologies). After incubation in blocking solution, the PVDF membranes were treated with diluted rabbit anti-*Cldn14*, *Cldn16*, and *Cldn19* (laboratory-generated); rabbit anti-*Trpv5* (CAT21-A; Alpha Diagnostic); mouse anti-*Calbindin-D28k* (Sigma); rabbit anti-phospho-p44/42 (Thr202/Tyr204; Cell Signaling Technology, Inc.); rabbit anti-CREB phospho-Ser133 (Assay Biotechnology); or mouse β -actin (Sigma). Horseradish peroxidase-conjugated anti-rabbit or mouse IgG was used as the secondary antibody (Jackson ImmunoResearch Laboratories), and signal was detected by Amersham ECL Prime Western Blotting Detection Reagent (GE Healthcare).

Immunofluorescence. Kidney tissues were dissected, fixed in 10% neutralized formalin, and embedded in paraffin or optimal cutting temperature compound (Sakura, Inc.). Five-micrometer sections were blocked with 0.1% BSA, 0.02% saponin, and 5% normal serum from species matching the labeled secondary antibodies. Sections were incubated with primary antibodies at $4^\circ C$ overnight. Alexa Fluor-conjugated secondary antibodies were used for immunofluorescence visualization (Life Technologies). The primary antibodies were rabbit anti-Tamm-Horsfall Glycoprotein (BTI), rabbit anti-*Cldn14* (laboratory-generated), rabbit anti-Aquaporin 2 (Novus Biologicals LLC), fluorescein-labeled *Lotus tetragonolobus* Lectin (LTL; Vector), rabbit anti-*Trpv5* (CAT21-A; Alpha Diagnostic), mouse anti-*Calbindin-D28k* (Sigma), and rabbit anti-RFP (Rockland).

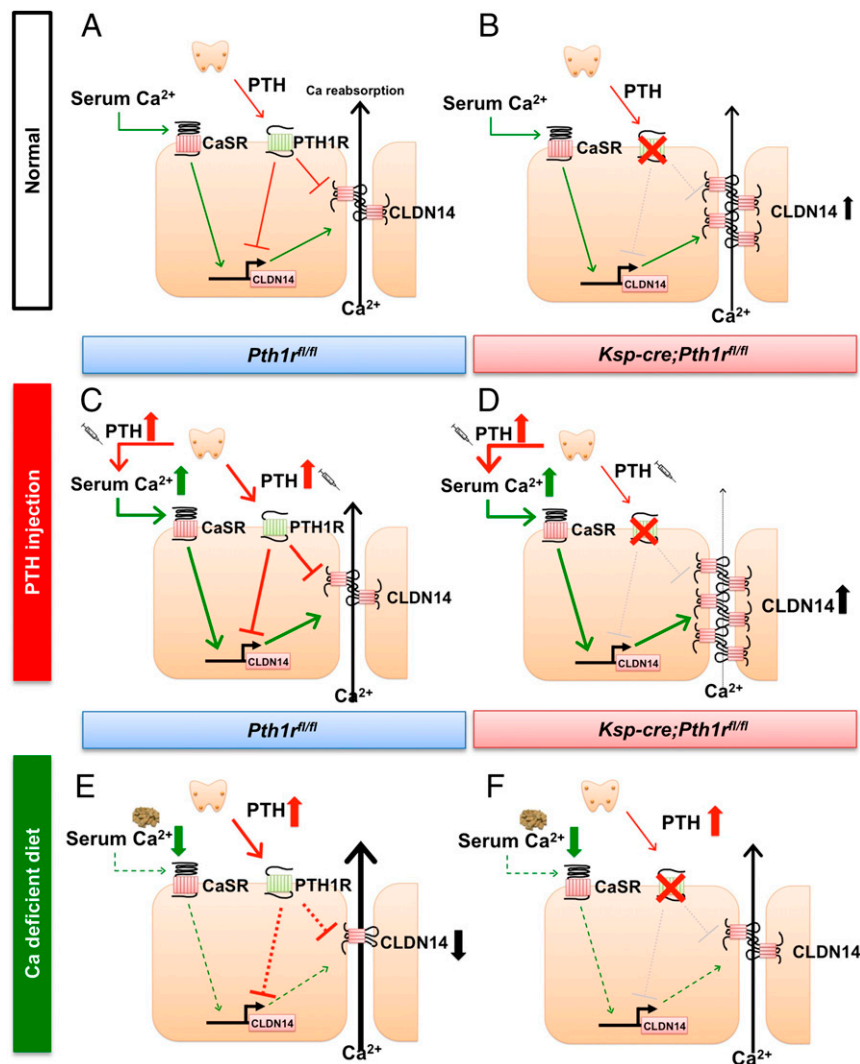


Fig. 7. Summary of findings is illustrated in a diagram. (A and B, Normal) Under healthy physiological conditions, with normal serum calcium and PTH levels, paracellular calcium transport is balanced by a combination of PTH1R and CaSR signaling. (A) On one hand, PTH can directly suppress *Cldn14* in the TAL to enhance paracellular Ca^{2+} reabsorption. On the other hand, PTH induces serum calcium and activation of the CaSR in the kidney, leading to an induction of *Cldn14* expression and thereby blocking paracellular Ca^{2+} reabsorption. A tight regulation between those two actions is critical to assure a balance in paracellular Ca^{2+} transport. (B) Deletion of PTH1R signaling in the TAL results in a loss of the suppressive effects of PTH on *Cldn14*, favoring the stimulation of *Cldn14* expression by calcium and resulting in hypercalciuria (decreasing Ca^{2+} reabsorption). (C and D, PTH injection) (C) Injection of PTH into mice increases serum calcium and CaSR signaling to induce *Cldn14* expression. An elevation in *Cldn14* levels leads to increased urinary Ca^{2+} wasting. PTH can directly suppress *Cldn14* expression in the TAL to stimulate paracellular Ca^{2+} reabsorption to balance its indirect effects on *Cldn14* via the CaSR. This dual action of PTH thus forms a mechanism for properly maintaining renal Ca^{2+} homeostasis in the TAL. (D) Loss of the suppressive function of PTH on *Cldn14* upon higher serum PTH levels leads to very high levels of *Cldn14*, causing severe urinary Ca^{2+} loss. (E and F, Ca^{2+} -deficient diet) (E) CaSR responds to low serum calcium levels by lowering its usual induction of *Cldn14* expression to preserve Ca^{2+} reabsorption. Low serum calcium levels also lead to a rise in serum PTH levels, which additionally suppress *Cldn14*, resulting in further conservation of calcium. (F) Loss of PTH1R signaling eliminates the suppression of *Cldn14* by PTH, thereby leaving some *Cldn14* expression intact.

Flow Cytometry. Renal cells expressing Tomato protein were isolated from *Ksp-cre;Tomato^{fl/+};Pth1r^{+/+}* or *Ksp-cre;Tomato^{fl/+};Pth1r^{fl/fl}* mice. Cells were trypsinized into a single-cell suspension, counted, and washed with PBS supplemented with 5% BSA. Cell fixation and staining with an anti-*Cldn14* antibody were performed using a FIX & PERM Cell Fixation & Permeabilization Kit (Life Technologies) according to the manufacturer's protocol. Cells were processed for flow cytometry analysis on a Becton Dickinson SORP LSR II instrument, and data were analyzed with CELLQuest Pro software (BD). For the detection of Tomato and *Cldn14*, Tomato-mCherry and *Cldn14*-FITC were used, respectively.

Time-Lapse Microscopy and 3D Reconstruction Image. Full-length claudins were cloned into the pEGFP vector (Clontech): mouse *Cldn14* (AF314089), human *CLDN16* (AF152101), and human *CLDN19* (BC030524). The pcDNA3-hPTH1R-DsRed plasmid was kindly provided by Thomas J. Gardella, Massachusetts General Hospital (43).

Cells were cultured in DMEM with 10% FBS, 4.5 g/L D-glucose, 584 mg/L L-glutamine, 110 mg/L sodium pyruvate, 100 U/mL penicillin, and 100 $\mu\text{g}/\text{mL}$ streptomycin. Transient transfections were performed using PolyJet In Vitro DNA Transfection Reagent (SigmaGen Laboratories) according to the manufacturer's protocol. After geneticin selection, DsRed and GFP double-positive cells were sorted by a FACSAria cell sorter (Becton Dickinson), collected in new tubes, and cultured in regular culture media. Cells were placed on 35-mm, no. 1.5 glass-bottomed culture dishes (In Vitro Scientific) for 2 d before imaging. Time-lapse microscopy was performed using a VivaView incubator fluorescence microscope (Olympus). Z-stack serial images were obtained by means of an Olympus FV1200 laser confocal microscope. Three-dimensional reconstruction, look-up table, and surface plot analyses were performed using ImageJ software (NIH) to investigate tight-junction protein localization on cell-cell junctions.

Statistical Analyses. All statistical analyses were performed using GraphPad Prism 5 for Windows (GraphPad Software, Inc.). Variables were

tested by either a two-tailed *t* test or Tukey test. Values were expressed as mean \pm SEM unless otherwise stated. A *P* value <0.05 was considered significant.

ACKNOWLEDGMENTS. We thank Tatsuya Kobayashi (Massachusetts General Hospital) for providing PTH1R flox mice, Thomas J. Gardella (Massachusetts

General Hospital) for providing pcDNA3-hPTH1R-DsRed plasmid, Henry Kronenberg (Massachusetts General Hospital) for helpful discussion, and all of the B.L. laboratory members for scientific discussion. This study was supported by NIH Grant DK097105. T.S was supported, in part, by the Harvard School of Dental Medicine Dean's Scholarship and the Uehara Memorial Foundation Research Fellowship.

1. Peacock M (2010) Calcium metabolism in health and disease. *Clin J Am Soc Nephrol* 5: 523–530.
2. Coe FL, Worcester EM, Evan AP (2016) Idiopathic hypercalciuria and formation of calcium renal stones. *Nat Rev Nephrol* 12:519–533.
3. Bihl G, Meyers A (2001) Recurrent renal stone disease—advances in pathogenesis and clinical management. *Lancet* 358:651–656.
4. Painter SE, Kleerekoper M, Camacho PM (2006) Secondary osteoporosis: A review of the recent evidence. *Endocr Pract* 12:436–445.
5. Hudec SM, Camacho PM (2013) Secondary causes of osteoporosis. *Endocr Pract* 19:120–128.
6. Polymeris A, Michalakos K, Sarantopoulou V (2013) Secondary osteoporosis - an endocrinological approach focusing on underlying mechanisms. *Endocr Regul* 47:137–148.
7. Topala CN, Bindels RJ, Hoenderop JG (2007) Regulation of the epithelial calcium channel TRPV5 by extracellular factors. *Curr Opin Nephrol Hypertens* 16:319–324.
8. Toka HR (2014) New functional aspects of the extracellular calcium-sensing receptor. *Curr Opin Nephrol Hypertens* 23:352–360.
9. Gong Y, et al. (2012) Claudin-14 regulates renal Ca^{++} transport in response to CaSR signalling via a novel microRNA pathway. *EMBO J* 31:1999–2012.
10. Weber S, et al. (2001) Novel paracellin-1 mutations in 25 families with familial hypomagnesemia with hypercalciuria and nephrocalcinosis. *J Am Soc Nephrol* 12:1872–1881.
11. Konrad M, et al. (2006) Mutations in the tight-junction gene claudin 19 (CLDN19) are associated with renal magnesium wasting, renal failure, and severe ocular involvement. *Am J Hum Genet* 79:949–957.
12. Wilcox ER, et al. (2001) Mutations in the gene encoding tight junction claudin-14 cause autosomal recessive deafness DFNB29. *Cell* 104:165–172.
13. Thorleifsson G, et al. (2009) Sequence variants in the CLDN14 gene associate with kidney stones and bone mineral density. *Nat Genet* 41:926–930.
14. Guha M, et al. (2015) Polymorphisms in CaSR and CLDN14 genes associated with increased risk of kidney stone disease in patients from the eastern part of India. *PLoS One* 10:e0130790.
15. Kurokawa K (1996) How is plasma calcium held constant? Milieu interieur of calcium. *Kidney Int* 49:1760–1764.
16. Ureña P, et al. (1993) Parathyroid hormone (PTH)/PTH-related peptide receptor messenger ribonucleic acids are widely distributed in rat tissues. *Endocrinology* 133:617–623.
17. Abou-Samra AB, et al. (1992) Expression cloning of a common receptor for parathyroid hormone and parathyroid hormone-related peptide from rat osteoblast-like cells: A single receptor stimulates intracellular accumulation of both cAMP and inositol trisphosphates and increases intracellular free calcium. *Proc Natl Acad Sci USA* 89:2732–2736.
18. Loupy A, et al. (2012) PTH-independent regulation of blood calcium concentration by the calcium-sensing receptor. *J Clin Invest* 122:3355–3367.
19. Gong Y, Hou J (2014) Claudin-14 underlies Ca^{++} -sensing receptor-mediated Ca^{++} metabolism via NFAT-microRNA-based mechanisms. *J Am Soc Nephrol* 25:745–760.
20. Dimke H, et al. (2013) Activation of the $\text{Ca}(2+)$ -sensing receptor increases renal claudin-14 expression and urinary $\text{Ca}(2+)$ excretion. *Am J Physiol Renal Physiol* 304:F761–F769.
21. Lupp A, et al. (2010) Immunohistochemical identification of the PTHR1 parathyroid hormone receptor in normal and neoplastic human tissues. *Eur J Endocrinol* 162:979–986.
22. Toka HR, et al. (2012) Deficiency of the calcium-sensing receptor in the kidney causes parathyroid hormone-independent hypocalciuria. *J Am Soc Nephrol* 23:1879–1890.
23. Suzuki T, Hara H (2006) Diffructose anhydride III and sodium caprate activate paracellular transport via different intracellular events in Caco-2 cells. *Life Sci* 79:401–410.
24. Sugibayashi K, Onuki Y, Takayama K (2009) Displacement of tight junction proteins from detergent-resistant membrane domains by treatment with sodium caprate. *Eur J Pharm Sci* 36:246–253.
25. Jilka RL (2007) Molecular and cellular mechanisms of the anabolic effect of intermittent PTH. *Bone* 40:1434–1446.
26. Blaine J, Chonchol M, Levi M (2015) Renal control of calcium, phosphate, and magnesium homeostasis. *Clin J Am Soc Nephrol* 10:1257–1272.
27. Kousteni S, Bilezikian JP (2008) The cell biology of parathyroid hormone in osteoblasts. *Curr Osteoporosis Rep* 6:72–76.
28. van Abel M, et al. (2005) Coordinated control of renal $\text{Ca}(2+)$ transport proteins by parathyroid hormone. *Kidney Int* 68:1708–1721.
29. de Groot T, et al. (2009) Parathyroid hormone activates TRPV5 via PKA-dependent phosphorylation. *J Am Soc Nephrol* 20:1693–1704.
30. Cha SK, Wu T, Huang CL (2008) Protein kinase C inhibits caveolae-mediated endocytosis of TRPV5. *Am J Physiol Renal Physiol* 294:F1212–F1221.
31. de Groot T, et al. (2011) Molecular mechanisms of calmodulin action on TRPV5 and modulation by parathyroid hormone. *Mol Cell Biol* 31:2845–2853.
32. Hoover RS, Tomilin V, Hanson L, Pochynuk O, Ko B (2016) PTH modulation of NCC activity regulates TRPV5 $\text{Ca}2+$ reabsorption. *Am J Physiol Renal Physiol* 310:F144–F151.
33. Bapty BW, et al. (1998) Extracellular $\text{Mg}2(+)$ - and $\text{Ca}2(+)$ -sensing in mouse distal convoluted tubule cells. *Kidney Int* 53:583–592.
34. Graca JA, et al. (2016) Comparative expression of the extracellular calcium-sensing receptor in the mouse, rat, and human kidney. *Am J Physiol Renal Physiol* 310:F518–F533.
35. Hoenderop JG, et al. (2001) Calcitriol controls the epithelial calcium channel in kidney. *J Am Soc Nephrol* 12:1342–1349.
36. Ikari A, et al. (2006) Phosphorylation of paracellin-1 at Ser217 by protein kinase A is essential for localization in tight junctions. *J Cell Sci* 119:1781–1789.
37. Van Itallie CM, Gambling TM, Carson JL, Anderson JM (2005) Palmitoylation of claudins is required for efficient tight-junction localization. *J Cell Sci* 118:1427–1436.
38. Hoenderop JG, Nilius B, Bindels RJ (2005) Calcium absorption across epithelia. *Physiol Rev* 85:373–422.
39. Robinson-Cohen C, et al. (December 7, 2016) Genetic variants associated with circulating parathyroid hormone. *J Am Soc Nephrol*, 10.1681/ASN.2016010069.
40. Hou J (2013) The role of claudin in hypercalciuric nephrolithiasis. *Curr Urol Rep* 14:5–12.
41. Olason H, et al. (2012) Targeted deletion of Klotho in kidney distal tubule disrupts mineral metabolism. *J Am Soc Nephrol* 23:1641–1651.
42. Kobayashi T, et al. (2002) PTHrP and Indian hedgehog control differentiation of growth plate chondrocytes at multiple steps. *Development* 129:2977–2986.
43. Maeda A, et al. (2013) Critical role of parathyroid hormone (PTH) receptor-1 phosphorylation in regulating acute responses to PTH. *Proc Natl Acad Sci USA* 110:5864–5869.